Preparation and characterization of Al_2O_3-based ceramic cores by binder jetting composite powder curing inorganic binder

Liu Jing-fei, * Yang Li, Xu Zi-zhen, Fan Zi-tian

State Key Laboratory of Materials Processing and Die & Mould Technology, School of Materials Science and Engineering, Huazhong University of Science and Technology, Wuhan 430074, China)

Abstract: Binder jetting can efficiently manufacture complex Al_2O_3-based ceramic components. However, the existing organic binder systems not only require a relatively high curing temperature, but also have a relatively large shrinkage rate of ceramic samples after high-temperature sintering. In this study, Al_2O_3 powder, silicate powder and powder curing additives are used as raw materials to prepare the green bodies through binder jetting. After curing at room temperature, the green bodies are degreased and sintered to obtain Al_2O_3-based ceramic core. The effects of the proportion of inorganic binders and curing agents and sintering temperatures on the properties of Al_2O_3-based ceramic cores are study. The results show that when the addition amount of silicate powder is 3 wt%, the bending strength after sintering at 1500 ℃ is 10.77 MPa, which meets the casting requirements.

Key words: Binder jetting; Inorganic binder; Powder curing agent; Al_2O_3; Ceramic cores

1 Introduction

Additive manufacturing (AM) technology are known as 3D printing technology, which can be traced back to the 1980s. It is designed to meet the professional requirements of complex structure preparation and rapid prototyping. Nowadays, it has become a universal technical platform in the fields of computer-aided design and rapid manufacturing[1]. AM technology is widely applied in the custom production of metal, ceramic and polymer materials as well as the rapid prototyping of complex parts [2-3], and it can achieve efficient moldless forming [4]. Therefore, AM technology has been widely applied in multiple fields such as healthcare, automobiles, aerospace, and construction [5-6].

Among them, binder jetting (BJ) has the advantages of fast forming speed, short production cycle and low material cost. It has been applied to the production of complex structures [7-9]. Yang et al. [10] were able to manufacture complex Al_2O_3-based ceramic components economically and efficiently by BJ. The bending strength and sintering relative density of the prepared Al_2O_3-based ceramics reached 113.79 MPa and 78.13 % respectively. When Mitra et al. [11] used furan resin binders, the mechanical strength of the sand mold could be enhanced by increasing the curing temperature and time. Bryant et al. [12] used the BJ process with furan binder, which could improve the mechanical strength of the sand mold by optimizing the parameters. However, the existing BJ mostly adopts organic binders, which not only require a relatively high curing temperature and have a large shrinkage rate after sintering, but also cause considerable pollution to the environment [13-15].

Over the past few decades, many efforts have been focused on specifically optimizing BJ processing parameters or material systems. However, there are relatively few studies on the influence of inorganic binder systems on the properties of ceramic samples [16-17]. Heng et al. has developed a new type of inorganic metal salt binder for enhancing the density and mechanical properties of bonded jetted tungsten-based alloys. The results show that the use of AMT binder can significantly increase the density and compressive strength of the green and pre-treated parts, and achieve sintering densification at a lower temperature [18]. Jiang et al. prepared starch-based binders using sodium alginate and polyvinylpyrrolidone as additives [19]. In a word, it is important to develop an inorganic binder suitable for the preparation of precision casting ceramics [20-21].

In this study, an in-situ dissolution and curing BJ process using silicate powder and water-based solvents is proposed to prepare the Al_2O_3-based ceramic cores with excellent performance. In addition, the effects of the addition amount of silicate powder and temperature on the Al_2O_3-based ceramic cores are studied.

2 Materials and methods

2.1 Raw materials and process

Al_2O_3 (Zhengzhou Green Energy Environmental Protection Co., LTD.), silicate powder (Henan Borun

Casting Materials Co., LTD.) and powder curing agent (Hebei Enyi Metal Materials Co., LTD.) were used as raw materials. The microscopic morphology is shown in **Figure 1**. The water-based binder (E115) is provided by Wuhan Easy Technology Co., LTD. First, Al_2O_3, silicate powder and powder curing agent are pre-mixed through a mixer as the base material. Printing was carried out using jet bonding forming equipment. The printing layer thickness was 0.04 mm, the inkjet volume was 55 %, and the model size was 50 mm × 10 mm × 8 mm. After printing, the green body and the powder bed need to be left to stand and cure at room temperature for 24 hours. And then, the green body was taken out and the surrounding powder was cleared. Subsenquently, high-temperature sintering was carried out directly at 1300 ℃, 1400 ℃ and 1500 ℃ for 3 hours respectively. After cooling with the furnace, the samples were obtained. The process flow is shown in **Figure 2**.

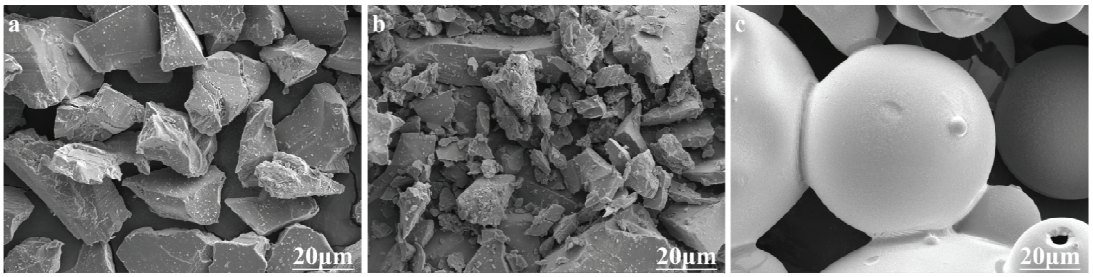

Figure. 1. Microstructure of the raw materials: (a) Al_2O_3; (b) Silicate powder; (c) Powder curing agent.

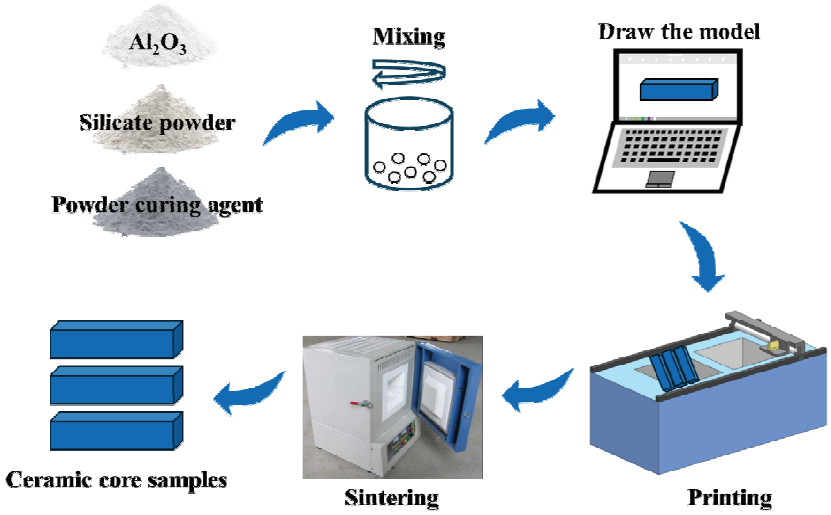

Figure. 2. Illustration of the preparation process of Al_2O_3-based ceramic cores.

2.2 Evaluation methods

The calculation formula of the shrinkage rate (φ) of the specimen is:

$$\varphi = \frac{l_0 - l_1}{l_0} \times 100\ \% \qquad (1)$$

In the formula, l_0 represents the width of the sample before sintering, and l_1 represents the width of the sample after sintering. The MTS810 universal testing machine was used to test the bending strength of the samples by the three-point bending method. The span of the testing machine is set at 30 mm, and the displacement speed of the punch is set at 0.05 mm/min. The bulk density (ρ_b) and apparent porosity (P_a) of the samples were tested by the Archimedes displacement method:

$$\rho_b = \frac{m_2 - m_0}{m_2 - m_1} \times \rho_{H_2O} \qquad (2)$$

$$P_a = \frac{m_0}{m_2 - m_1} \times 100\ \% \qquad (3)$$

In the formula, m_0 represents the mass of the dried sample, m_1 represents the mass of the sample measured in water, and m_2 represents the mass of the sample after absorbing water. The microscopic morphology of samples was observed using the scanning electron microscope - RISE-CLARA system. The surface contour undulations of the ceramic samples were tested and characterized using the ultra-depth-of-field three-dimensional microscope (EasyZoom5 3D).

3 Results and discussion

3.1 Physical property

Figure 3 shows the effect of different silicate addition amounts on the bending strength of green bodies. After curing at room temperature for 24 hours,

the results show that with the increase of the addition amount of silicate, the bending strength of the green body first increases and then decreases. This is because the silicate as a binder promotes the contact between the ceramic powder and the powder curing agent, making the body more dense. When the addition amount of silicate is moderate, it can effectively fill the voids between ceramic particles and improve the bending strength of the green body. However, when the addition amount of silicate exceeds 3wt%, a large number of pores and cracks will form in the green body. These defects will significantly reduce the bonding strength between powder particles, thereby leading to a decrease in the bending strength of the green body. In this study, when the addition amount of silicate is 3 wt%, the bending strength of the green body after curing at room temperature for 24 hours reaches 1.96 MPa.

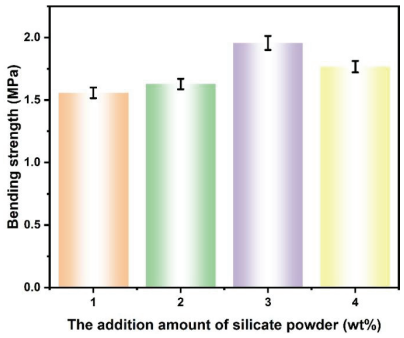

Figure. 3. Effect of silicate addition amount on the bending strength of green bodies.

Figure 4 shows the evolution laws of mechanical properties of samples with different silicate contents under different sintering temperature conditions. With the increase of sintering temperature, the shrinkage rate, bending strength and bulk density of the sample show a trend of increasing first and then decreasing, while the porosity shows the opposite changing trend. First, the impurity oxides present in the raw materials are conducive to the sintering of the samples. They can accelerate the chemical reactions inside the samples and are conducive to the formation of a more compact structure. Second, as the sintering temperature increases, the bonding between powder particles gradually strengthens, the size of ceramic grains significantly increases, and the pores gradually close. This series of microstructure changes indirectly leads to an increase in the shrinkage rate, bending strength and bulk density of the samples. However, when the addition amount of silicate powder exceeds 3 wt%, the silicate powder will decompose and release gas during the sintering process. This is not conducive to the sintering densification of the sample. And it will also form a large number of pores inside the sample, thereby leading to a decrease in volume density and bending strength.

In summary, the optimal addition amount of silicate powder is 3 wt%. Under these conditions, the shrinkage rate of the ceramic green body at 1300 ℃-1500 ℃ is 1.12 %-3.48 %, the bulk density is 1.72 g·cm^{-3}-1.89 g·cm^{-3}, the apparent porosity is 53.59 %-58.02 %, and the bending strength is 2.37 MPa-10.77 MPa.

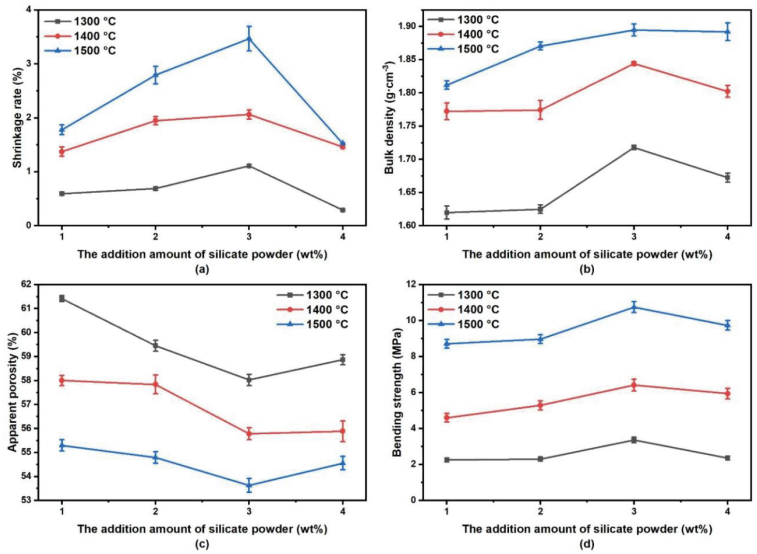

Figure. 4. Effects of silicate powder content and sintering temperature on physical properties of samples:

(a) shrinkage rate; (b) bulk density; (c) apparent porosity; (d) bending strength.

3.2 Microstructure

The microscope images of the fracture morphology of Al_2O_3-based ceramic cores with different silicate powder addition amounts at a sintering temperature of 1400 ℃ are shown in **Figure 5**. It can be seen from

Figure 5 that after sintering at a of 1400 ℃, the average particle size of Al_2O_3-based ceramic cores did not change significantly with the increase of the addition amount of silicate powder. However, a layer of newly formed micron-sized silicate particles is deposited on the surface of the alumina particles after heat treatment. These tiny silicate particles fill the pores in the Al_2O_3 powder layer. Further observation revealed that the porosity of Al_2O_3-based ceramic cores decreased with the increase of the addition amount of silicate. This change indicates an increase in the densification degree of the internal structure of the material and leads to an increase in shrinkage rate. In addition, at 1400 ℃, the increase in the addition amount of silicate promotes the formation of more neck bonding between the newly generated micron-sized silicate particles and the Al_2O_3 particles. These neck bonds closely connect the originally dispersed Al_2O_3 particles, not only effectively limiting the shrinkage during the sintering process, but also significantly enhancing the bending strength of Al_2O_3-based ceramic cores.

In conclusion, reasonably regulating the addition amount of silicate can effectively improve the microstructure of Al_2O_3-based ceramic cores and enhance their overall performance.

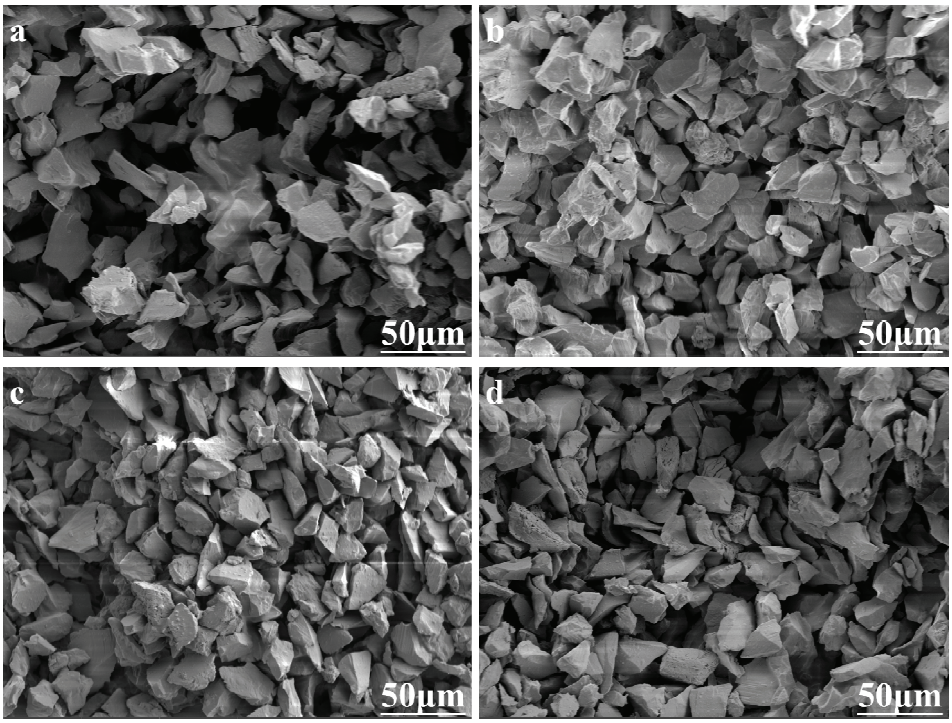

Figure. 5. Microstructure images of the samples with different amounts of silicate at 1400 °C:

(a~d) represents the amount of silicate added as 1 wt%, 2 wt%, 3 wt% and 4 wt% in order.

Figure 6 shows the fracture morphology of the sample with an addition amount of 3 wt% of silicate within the sintering temperature range of 1300 °C to 1500 °C. With the gradual increase of sintering temperature, the interaction between powder particles is significantly strengthened, and chemical bond mergers begin to form, undergoing structural rearrangement. With the gradual increase of sintering temperature, the interaction between powder particles began to form chemical bonds and undergo structural rearrangement. This process is accompanied by the gradual disappearance of large pores and the reduction of the total volume of pores. With the further increase of sintering temperature, the material transport process becomes more active. The interfaces of ceramic particles continue to develop and expand. The original pores gradually shrink and deform under the continuous heat treatment effect, and eventually transform into isolated closed pores. Meanwhile, the particle interface begins to migrate. Along with the growth of the particles, the pores migrate to the particle interface and disappear accordingly. This process greatly enhances the bulk density of the sample. The increase of bulk density reduces the internal defects of the material and enhances the bonding strength between the particles, thus significantly improving the bending strength of the sample.

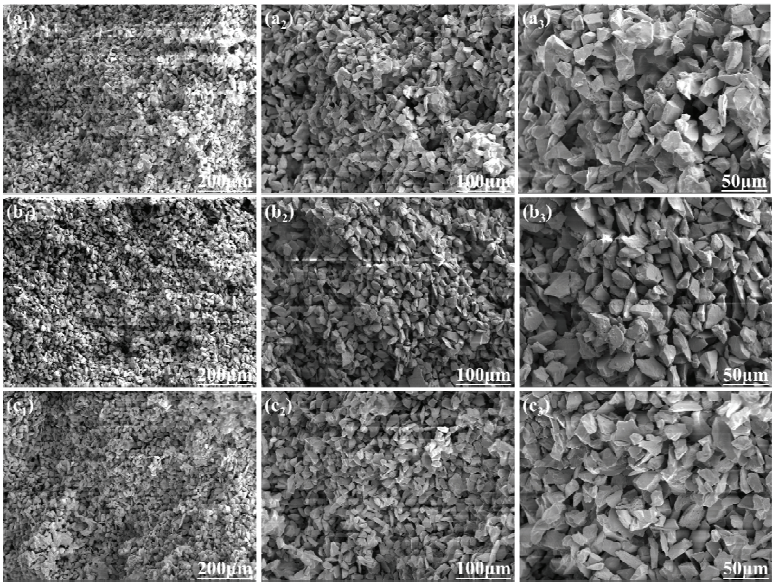

Figure. 6. When the addition of silicate powder is 3wt%, the microstructure images of the samples with different sintering temperatures: (a~c) represents the sintering temperature of 1300 °C, 1400 °C and 1500 °C in order; the subscript (1~3) represent different magnifications of 500X, 1000X, and 2000X in order.

3.3 Surface roughness

Figure 7 shows the influence of different silicate addition amounts (1 wt%-4 wt%) and sintering temperatures (1300 ℃-1500 ℃) on the roughness of the specimens. At 1400 ℃, the increase in the addition amount of silicate leads to a decrease in the surface roughness of the top and side surfaces of the sample first and then an increase. At a lower addition amount of silicate, there is not enough binder to provide binding force for the powder particles. Some powder partially fell off the surface of the sample, resulting in an increase in surface roughness. When the addition amount of silicate is higher than 3 wt%, the excessive powder combines with the surface, resulting in surface expansion and poor surface roughness. In summary, when the addition amount of silicate powder is 3 wt%, the surface roughness of the sample shows the best performance. Specifically, after heat treatment at a sintering temperature of 1400 ℃, the top roughness of the sample reached 12.8 μm, and the side roughness was 27.2 μm.

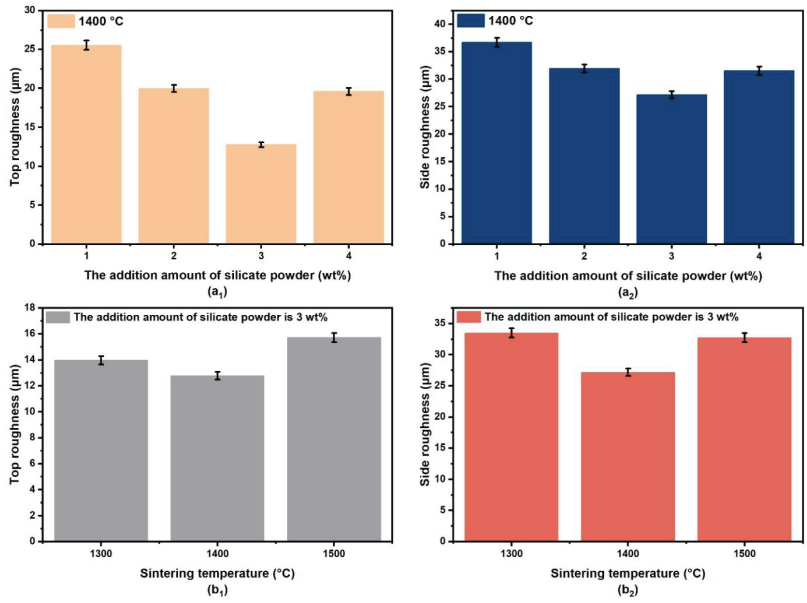

Figure. 7. Effects of different addition amount of silicate powder and sintering temperature on the surface roughness of the samples: (a~b) represents the different addition amount of silicate powder and sintering temperature in order; the subscript (1~2) represents the top roughness and side roughness in order.

As shown in **Figure 8**, the addition amount of silicate has a significant effect on the three-dimensional super-depth-of-field surface morphology of the sample at 1400 ℃. Compared with the side surface, the top surface of the sample is more uniform and smooth after sintering. This is because during the sintering process, the top surface is heated more evenly, which promotes the uniform growth and arrangement of grains and reduces the surface roughness. Further observation revealed that with the increase of the addition amount of silicate, the color of the three-dimensional super-depth-of-field surface morphology gradually changed from orange-red to sky green. This indicates that with the increase of the addition amount of silicate, the roughness of both the side surface and the top surface decreases. Because silicate can promote the densification process of the material at high temperature to reduce the formation of pores and cracks, so that the surface is smoother. In this study, when the addition amount of silicate was 3 wt%, the surface roughness of the samples performed the best.

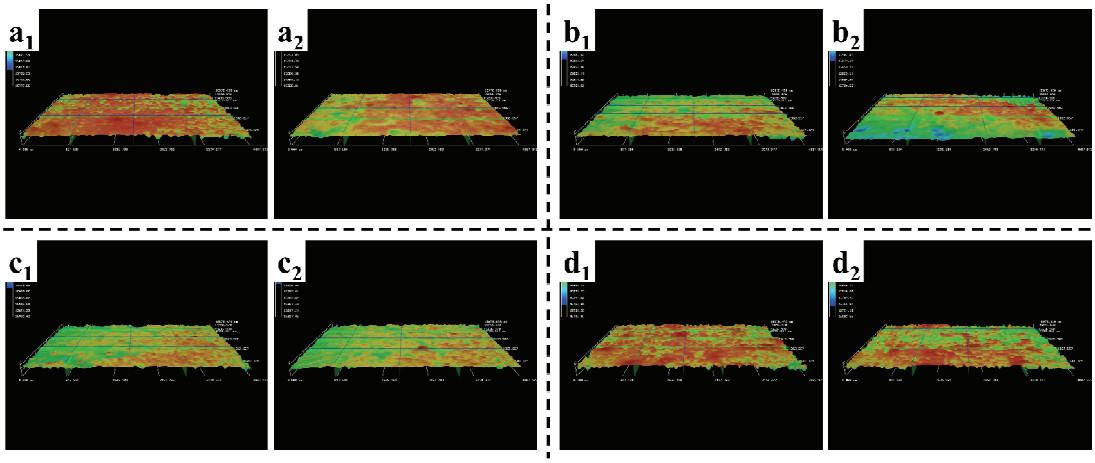

Figure. 8. Ultra-depth 3D microscope images of the samples with different amounts of silicate:

(a~d) represents the amount of silicate powder added is 1 wt%, 2 wt%, 3 wt% and 4 wt% in order; (1~2) represent top roughness and side roughness respectively.

4 Conclusions

(1) Based on the binder jetting of Al_2O_3-based ceramic cores, the properties of the samples under different silicate addition amounts and sintering temperatures were characterized and analyzed. The results show that an appropriate amount of silicate can effectively promote the sintering densification process and significantly improve the bending strength and bulk density of the samples. However, when excessive silicate is added, the bulk density will decrease, thereby reducing the bending strength. In this study, when the addition amount of silicate powder is 3 wt%, the bending strength after sintering at 1500 ℃ is 10.77 MPa, which meets the casting requirements. Moreover, the shrinkage rate of the sample after sintering is only 3.48 %.

(2) With the increase of the amount of silicate added, the connection and contact area between the particles in the sample expand to form more neck connections, thus significantly enhancing the bending strength. In addition, with the increase of the addition amount of silicate, the surface roughness of the top and side surfaces of the sample first decreases and then increases. In this study, when the addition amount of silicate powder was 3 wt%, the top roughness was 15.7 μm and the side roughness was 32.8 μm after sintered at 1500 ℃.

References

[1] K. Zhou, R. R. Zhao, H. J. Qi, Special Issue Editorial: Advanced Materials for Additive Manufacturing[J]. Advanced Materials, 2024, 36: 2410446.

[2] K. P. Akhilesh, K. M. Amar, M. Manjusri, Additive manufacturing technology of polymeric materials for customized products: recent developments and future prospective[J]. RSC Advances, 2021, 11: 36398.

[3] M. D. Gao, L. Lei, Q. Y. Wang, et al, Feature-based energy consumption quantitation strategy for complex additive manufacturing parts[J]. Energy, 2024, 297: 131249.

[4] M. Alejandro, A. D. Jose, M. Iván, et al, Improvements in Injection Moulds Cooling and Manufacturing Efficiency Achieved by Wire Arc Additive Manufacturing Using Conformal Cooling Concept[J]. Polymers, 2024, 16: 3057.

[5] H. A. Abdul, G. O. Abdul, A. Adnan, et al, Additive

manufacturing in the aerospace and automotive industries: Recent trends and role in achieving sustainable development goals[J]. Ain Shams Engineering Journal, 2023, 14: 102516.

[6] J. Wang, C. M. Shao, Y. T. Wang, et al, Microfluidics for Medical Additive Manufacturing[J]. Engineering, 2020, 6: 1244-1257.

[7] E. Donval, M. Schneider, H. G. Strele, et al, A directional contraction method to model sand-based binder jet 3D printed materials[J]. International Journal of Solids and Structures, 2025, 312: 113260.

[8] M. Ziaee, N. B. Crane, Binder jetting: A review of process, materials, and methods[J]. Additive Manufacturing, 2019, 28: 781-801.

[9] S. J. Huang, C. S. Ye, H. P. Zhao, et al, Additive manufacturing of thin alumina ceramic cores using binder-jetting[J]. Additive Manufacturing, 2019, 29: 100802.

[10] Z. Y. Yang, L. Yang, P. L. Wang, et al, Effect of sintering aid combined vacuum infiltration on the properties of Al_2O_3-based ceramics via binder jetting[J]. Additive Manufacturing, 2024, 79: 103898.

[11] S. Mitra, D. C. Rodríguez, M. E. Mansori, The effect of ageing process on three-point bending strength and permeability of 3D printed sand molds[J]. The International Journal of Advanced Manufacturing Technology, 2018, 97: 1241-1251.

[12] N. Bryant, T. Frush, J. Thiel, et al, Influence of Machine Parameters on the Physical Characteristics of 3D-Printed Sand Molds for Metal Casting[J]. International Journal of Metalcasting, 2021, 15: 361-372.

[13] R. H. Dana, M. E. Mansori, Mechanical characterisation of anisotropic silica sand/furan resin compound induced by binder jet 3D additive manufacturing technology[J]. Ceramics International, 2020, 46: 17867-17880.

[14] F. Wang, X. H. Cui, Q. Yang, et al, Fabrication and posttreatment for inorganic binder jetting sand molds for casting[J]. Additive Manufacturing, 2023, 73: 103690.

[15] J. W. Zhao, X. L. Gong, X. J. Xiao, et al, Preparation of high-strength and low-shrinkage composite salt cores by binder jetting and vacuum impregnation[J]. Materials and Manufacturing Processes, 2024, 39: 2099-2110.

[16] Z. F. Zhang, L. Wang, L. T. Zhang, et al, Binder jetting 3D printing process optimization for rapid casting of green parts with high tensile strength[J]. China Foundry, 2021, 18: 335-343.

[17] E. M. Jimenez, D. M. Ding, L. S. Su, et al, Parametric analysis to quantify process input influence on the printed densities of binder jetted alumina ceramics[J]. Additive Manufacturing, 2019, 30: 100864.

[18] Y. H. Heng, Y. W. Mao, K. H. Feng, et al, Enhanced green density of binder jetted tungsten heavy alloys with an inorganic metal salt binder[J]. Journal of Materials Research and Technology, 2025, 35: 2226-2241.

[19] H. T. Jiang, X. H. Yang, H. Wang, Preparation and characterization of starch-based binders for binder jetting[J]. RSC Advances, 2024, 44: 32506.

[20] S. Tharmalingam, B. Nagasivamuni, S. Prateek, et al, A review on the progress and challenges of binder jet 3D printing of sand moulds for advanced casting[J]. Additive Manufacturing, 2021, 40: 101889.

[21] S. S. Wang, E. Liang, X. L. Han, et al, The Exploration of Ink Formulations in Binder Jet 3D Printing Drugs[J]. 3D Printing and Additive Manufacturing, 2024, 11: e1606-e1615.